Analysis and Assessment of Knowles' Partitioning in Many-Body Perturbation Theory

Journal:	*Journal of Chemical Theory and Computation*
Manuscript ID	ct-2024-00166x.R1
Manuscript Type:	Article
Date Submitted by the Author:	n/a
Complete List of Authors:	Gombás, András; ELTE TTK, Laboratory of Theoretical Chemistry Surjan, Peter; ELTE, Chemistry Szabados, Agnes; Eotvos Lorand Tudomanyegyetem Kemiai Intezet, Laboratory of Theoretical Chemistry

Analysis and Assessment of Knowles' Partitioning in Many-Body Perturbation Theory

András Gombás,* Péter R. Surján,* and Ágnes Szabados*

Laboratory of Theoretical Chemistry, Institute of Chemistry, Faculty of Science, ELTE Eötvös Loránd University, H-1518 Budapest 112, P.O.B. 32, Hungary

E-mail: gombasandras@student.elte.hu; peter.surjan@ttk.elte.hu; agnes.szabados@ttk.elte.hu

Abstract

A detailed analysis of a new partitioning in many-body perturbation theory recently proposed by Knowles (J. Chem. Phys. 156, 011101, 2022), termed 'perturbation adapted partitioning' (PAPT), is presented. Level-shift and orbital rotation effects are identified as gears of the zero-order Hamiltonian. These two components are examined separately, revealing that in themselves neither of the two are competitive with the combined effect. The success of PAPT can be attributed to determining a set of molecular orbitals and corresponding orbital energies that can systematically outperform the canonical orbitals and Koopmans' energies based Møller-Plesset partitioning.

The self-consistent version of the method is also tested in terms of energy and convergence. Previous numerical studies are further complemented with an application on an inherent multireference example and investigation of van der Waals interaction energies. In addition, a rigorous mathematical analysis of the consequence of the linear dependence of projection functions on the solution of the Knowles' equations is provided.

Introduction

As a reliable and cost-effective first approximation of the dynamical correlation energy, Møller-Plesset (MP)[1] partitioning based perturbation theory (PT) is ubiquitous in current day quantum chemical applications.[2,3] Its role is not always to provide a final answer, MP based correction often appears as part of more convoluted approximation strategies.[4–7] Early studies on the computationally efficient calculation of MP energies and derivatives date from the 80's[8,9] and the subject has been repeatedly seeing inspired new approaches.[10–23] Besides it prevalent use, limits of applicability of MP based PT has been also investigated thoroughly. Breakdown of low order approximations in the case of quasi-degeneracy was soon revealed.[24] Convergence of the MP series is a rather theoretical than practical question, which was the subject of several numerical studies.[25–28] Stunning numerical experience of divergence were explored with the help of analysis of complex functions[29–31] as well as inspection of matrix elements, especially zero-order excitation energies.[32]

Relying on the single determinantal Fockian as zero-order is a straightforward but not unique choice for correcting the Hartree-Fock (HF) approximation via PT. Several alternative partitionings have been explored, especially in view of the challenging cases of application. Malrieu e.g. argued on the superiority of the Epstein-Nesbet (EN)[33,34] partitioning over MP[35] and advocated the use of a mixture of the two in multireference situations.[36] It is well-known that the EN and MP partitionings are related by appropriate level-shifts at the zero-order.[37] The idea of arbitrary level-shift parameters introduced at zero-order and chosen by requiring that certain characteristic of the PT series improves is present in several studies.[38–49] Feenberg's scaling, operating with a single parameter[50,51] was harnessed in the same vein.[52] Optimization of all matrix elements of the zero-order Hamiltonian, i.e. not only those in the diagonal is a more difficult task, that has seen less attempts. Adopting a Hilbert-space based approach Adams constructed a block-diagonal structure for the zero-order[53] and showed properties reminiscent of a Feenberg scaled partitioning. The second-quantized formulation of a zero-order Hamiltonian corresponding to Adams's block-diagonal suggestion was put forward by Fink.[54] A computationally facile repartitioning, op-

erating with a specific, nondiagonal transformation formulated in the Hilbert-space was advocated by Dietz et al.[55] Choice for an effective one-body potential suitable for a zero-order operator was initiated by Kelly,[56,57] investigated by Bartlett and Silver[58] and used extensively by Freed when designing valence shell effective Hamiltonians on an ab initio basis.[59–61] Amplitude regularization in the Brillouin-Wigner framework, suggested by Head-Gordon, affecting orbitals in the occupied subspace[62,63] also falls in this category.

An important development was published recently by Knowles, suggesting a method termed perturbation adapted partitioning (PAPT),[64] which in the above context, represents an optimization of a full one-body zero-order Hamiltonian. Improved convergence properties of the new partitioning were demonstrated for some difficult cases identified earlier with MP.

The present study aims at broadening the range of numerical comparison, focusing on the performance of low order PT terms and showing alternative partitioning optimization techniques investigated formerly in our laboratory.

The fact that PAPT formulates a Brilloiun-theorem conserving zero-order lends a further perspective to the subject. The Knowles' partitioning can be considered a method that simultaneously optimizes HF orbitals and orbital energies to be used in a many-body PT expansion. Starting from the 60's, a vivid interest grew in PT on localized orbitals, concerning how to perform PT with localized orbitals[65,66] and conversely, finding localized orbitals that are most advantageous for developing a PT expansion for the correlation energy of the ground state.[67,68] Regarding the former, Pulay advocated the application of the MP partitioning,[8,9] while Kapuy conducted extensive studies on applying only the diagonal elements of the Fockian as zero-order and leaving all nondiagonal elements for perturbation.[69–74] Numerical comparison of low order PT terms obtained in localized orbitals invariably shows Pulay's approach outperforming Kapuy's. This means that the extra effort put into solving the PT equations with a nondiagonal zero-order pays off in the accuracy of the results. In addition, localized nature of the orbitals can be efficiently exploited to the extent that computational economy eventually favors localized orbitals over canonicals for large systems. Computational practice conveying an unequivocal message, Kapuy's approach was

largely abandoned, with some exceptions.[75–77]

As PAPT orbitals transform according to irreducible representations of the molecular point group, they are inherently nonlocal. Knowles' recent study nevertheless relates to the Kapuy-Pulay dilemma mentioned above, with raising the question whether a set of noncanonical HF orbitals may be advantageous not only for computational efficiency but also for the accuracy of the PT results. Taking this point of view we separate level-shift and orbital rotation component of PAPT and assess the performance of the two components separately. In particular, we examine whether a simpler, level-shift approach may offer results of comparable accuracy. We also test Kapuy's partitioning in PAPT orbitals, and inspect whether they fit in the general trend when compared with Pulay's approach, i.e. MP evaluated in PAPT orbitals in our case.

Theoretical background of the methods studied in this report is given in Section Theory. A subsection dwells on the separation of level-shift and orbital rotation, another subsection elaborates on some features of Knowles' partitioning, briefly mentioned in Ref.[64] A further subsection is devoted to the self-consistent solution of the PAPT equations, following the initiative of Ref.[64] Numerical assessments followed by concluding remarks in section Conclusion closes the paper.

Theory

One-body zero-order Hamiltonians

The Fockian corresponding to the closed shell determinant composed with canonical molecular orbitals

$$F = \sum_p \varepsilon_p E_p^p \tag{1}$$

represents the zero-order operator in the MP partitioning of PT. In the above E_q^p is the shorthand for generators of the unitary group

$$E_q^p = \sum_\sigma \varphi_{p\sigma}^\dagger \varphi_{q\sigma}^- \ ,$$

while orbital energies read as

$$\varepsilon_p = h_{pp} + \sum_j^{\mathrm{occ}} \left(2\langle\varphi_p\varphi_j|\varphi_p\varphi_j\rangle - \langle\varphi_p\varphi_j|\varphi_j\varphi_p\rangle\right) \tag{2}$$

with the $\langle 12|12\rangle$ convention adopted for two-electron integrals. Spatial part of canonical molecular orbitals is denoted by φ_p, latin indices $i, j, \ldots$ refer to occupied, $a, b, \ldots$ virtual and $p, q, \ldots$ generic orbitals and σ stands for the spin label.

Improving PT results by substitution of a set of orbital energies different from Eq. (2) in Eq. (1), and applying the thus produced one-body operator as zero-order has been investigated in several studies.[38,78–81] Such a tweak, termed level-shift, is a simple, special case of the more general partitioning optimization strategy where every matrix element $\overline{F}_{pq}$ of the one-body zero-order

$$\overline{F} = \sum_{pq} \overline{F}_{pq} E_q^p \tag{3}$$

is considered as parameter to be determined. Applying the constraint $\overline{F}_{ia} = \overline{F}_{ai} = 0$, only $\overline{F}_{ij}$ and $\overline{F}_{ab}$ are up to choice and the Brillouin-theorem remains valid. This approach can be regarded as seeking a set of occupied and virtual orbitals, ψ_p together with their associated orbital energies, $\overline{\varepsilon}_p$ facilitating to express the zero-order as

$$\overline{F} = \sum_p \overline{\varepsilon}_p \sum_\sigma \psi_{p\sigma}^\dagger \psi_{p\sigma}^- \ . \tag{4}$$

In fact, it has been pointed out that there is a one-to-one correspondence between the $\overline{F}_{ij}$ and $\overline{F}_{ab}$ matrix elements of a Brillouin-theorem complying one-body operator, Eq. (3) and the A_{pq} elements

of an arbitrary one-body operator introduced by Davidson to account for orbital localization at the HF level.[68,82] For a short recap on Davidson's A-matrix technique and the correspondence between $\overline{F}_{pq}$ and Davidson's A_{pq} see the Appendix. Though the general form of Eq. (3) allows for occupied-virtual mixing of orbitals, as applied in Bruecker's theory,[83,84] constraining the occupied-virtual matrix elements of $\overline{F}$ to be zero is more akin to a localization transformation, that conserves the Hartree-Fock determinant as eigenfunction of $\overline{F}$.

Diverting from a diagonal zero-order raises a technical issue in connection with evaluating PT terms. Redefined one-particle energies in Eq. (1) generate a mere shift in energy denominators and diagonal matrix elements of the perturbation operator, the latter from 3rd order on in energy. The expression in Eq. (3) is more complicated than level-shifts in the sense that it does not conserve the set of canonical orbitals as the eigenbasis of the zero-order. Therefore, as the PT expressions require to evaluate the effect of the inverse of the zero-order Hamiltonian at each successive order, one either has to work with a nondiagonal representation of $\overline{F}$ or turn to the new eigenbasis, c.f. Eq. (4). The former approach has been advocated by Pulay in the context of MP PT on the basis of localized orbitals.[8,9] With efficient linear equation solvers, this route is certainly more advantageous than the 5th power scaling integral transformation involved by Eq. (4).

While evaluating the inverse of $\overline{F}$ is a technical matter, there is also a conceptual question associated with Eqs. (1) and (3). Is it possible to separate and quantify the effect of level-shift and orbital rotation implied by Eq. (3)? A formal answer is provided in the rest of the Section. The expressions worked out below are used to quantify level-shift and orbital rotation ingredients of the PAPT approach in the Applications Section.

Level-shift component of Eq. (3)

Simplicity of level-shifts lies with conserving the original basis. Once a set of parameters $\overline{F}_{pq}$ are determined, it is straightforward to deduce the level-shift component, in accordance with Eq. (1),

as the effect of $\overline{F}_{pp}$ solely. The associated zero-order, reading as

$$\overline{F}^{\mathrm{LS}} = \sum_p \overline{F}_{pp}\, E_p^p \tag{5}$$

can be considered a working expression behind the method which will be labeled PAPT-LS.

Orbital rotation component of Eq. (3)

In order to identify the orbital rotation implied by $\overline{F}$, expression Eq. (4) is a suitable starting point. Applying Davidson's terminology, ψ_p are proper canonical orbitals to $\overline{F}$, meaning that the representation of $\overline{F}$ is diagonal. Obviously, an $\overline{F}$ to which a given set of ψ_p are proper canonical is nonunique, the value of $\overline{\varepsilon}_p$ being immaterial from this respect.

Let us approach the question from the point of view of Davidson's A-matrix, composed of elements A_{pq}. Consider the nondiagonal representation of the Fockian on the basis of ψ_p

$$F = \sum_{pq} F_{pq} \sum_\sigma \psi^\dagger_{p\sigma} \psi^-_{q\sigma} \tag{6}$$

and seek matrix A such that the resulting $\overline{F}$ is diagonal. This requirement fixes A_{pq} as[85]

$$A_{pq} = (-1)^{n_p}(N-1)F_{pq} \qquad \text{for } p \neq q \tag{7}$$

with n_p taking values 0 or 1 as the occupation number of spinorbital $\psi_{p\sigma}$ and N standing for the number of electrons in the system. Note that A_{pp} remains arbitrary.

As a result of Eq. (7), $\overline{F}_{pq}$ becomes zero for $p \neq q$, as can be checked based on the expressions of the Appendix. We argue that keeping $A_{pp} = 0$ corresponds to the minimal and necessary modification of F_{pq} in order to arrive at an $\overline{F}$ diagonal on the basis of $\psi_{p\sigma}$. Accordingly, the orbital rotation component of Eq. (3) is associated with $A_{pp} = 0$, resulting in

$$\overline{F}^{\mathrm{ROT}} = \sum_p F_{pp} \sum_\sigma \psi^\dagger_{p\sigma} \psi^-_{p\sigma} \tag{8}$$

where F_{pp} is the diagonal matrix element of the Fockian taken with $\psi_{p\sigma}$. The use of Eq. (8) as zero-order on the basis of localized orbitals has been extensively studied by Kapuy[69–73] and it was recently revisited by Subotnik and Head-Gordon.[77] From this point of view, a zero-order Hamiltonian of the form of Eq. (4) for which $\overline{\varepsilon}_p \neq F_{pp}$ can be considered a level-shifted Kapuy-partitioning.

The zero-order of Eq. (8) lies behind the method will be labeled PAPT-ROT below. Eigenbasis of $\overline{F}$ is constructed for the sake of analysis. Evaluation of PT expressions in noncanonical orbitals ψ_p is facilitated by integral dressing allowing to sidestep explicit construction of localization diagrams.[85]

Particulars of the PAPT equations

The incentive behind the PAPT equations for parameters $\overline{F}_{pq}$, as suggested by Knowles,[64] is that the zero-order operator should be as close as possible to the full Hamiltonian. This general idea is given a well-defined sense by evaluating the effect of both H and $\overline{F}$ on the first order wavefunction and equating certain projections of the two. Projecting functions, intuitively defined by Knowles[64] are contracted doubly excited configurations, reading

$$|\theta_{ij}^{+}\rangle = \sum_{abk} \left(c_{ab}^{ik} E_{jk}^{ab} + c_{ab}^{jk} E_{ik}^{ab} \right) |\mathrm{HF}\rangle \,, \tag{9a}$$

$$|\theta_{ab}^{+}\rangle = \sum_{ijc} \left(c_{ac}^{ij} E_{ij}^{bc} + c_{bc}^{ij} E_{ij}^{ac} \right) |\mathrm{HF}\rangle \,, \tag{9b}$$

where $|\mathrm{HF}\rangle$ stands for the Hartree-Fock determinant and expansion coefficients c_{ab}^{ij} of the first order MP wavefunction

$$\Psi^{(1)} = \sum_{ijab} c_{ab}^{ij} \, E_{ij}^{ab} \, |\mathrm{HF}\rangle \tag{10}$$

are given as

$$c_{ab}^{ij} \;=\; -\frac{1}{2}\,\frac{\langle\varphi_i\varphi_j|\varphi_a\varphi_b\rangle}{\varepsilon_a+\varepsilon_b-\varepsilon_i-\varepsilon_j}\,.$$

Note that indices $i,j,\ldots$ and $a,b,\ldots$ are restricted as mentioned above. Introducing the normal ordered form of operators $H_{\mathscr{N}} = H - \langle H\rangle$ and $\overline{F}_{\mathscr{N}} = \overline{F} - \langle\overline{F}\rangle$, with $\langle.\rangle$ referring to the expectation value with the Fermi vacuum, the PAPT equations read

$$\langle\theta_{ij}^{+}|\overline{F}_{\mathscr{N}}|\Psi^{(1)}\rangle \;=\; \langle\theta_{ij}^{+}|H_{\mathscr{N}}|\Psi^{(1)}\rangle \;\text{ for }\; i\le j\;, \tag{11a}$$

$$\langle\theta_{ab}^{+}|\overline{F}_{\mathscr{N}}|\Psi^{(1)}\rangle \;=\; \langle\theta_{ab}^{+}|H_{\mathscr{N}}|\Psi^{(1)}\rangle \;\text{ for }\; a\le b\;. \tag{11b}$$

Formulation of the equations with unitary generators is a minor difference with Ref.,[64] that does not alter the outcome. For the sake of consistent notation within the report, we use $\overline{F}$ for the zero-order operator denoted $\hat{\Lambda}$ in Ref.[64]

In terms of computational cost, PAPT is in league with MP3 and CCSD, exhibiting a formal $\mathscr{O}(6)$ scaling with the dimension of the one-particle basis. This stems from the rhs of Eq. (11), essentially requiring to construct the 2nd order wavefunction. With proper intermediers introduced, the more demanding terms feature $\sim n_{occ}^2 n_{virt}^4$ dependence.

On the rank of Eq. (11)

Assuming hermiticity of $\overline{F}$, the number of unknowns matches the number of equations in Eq. (11), given by $M = n_{occ}(n_{occ}+1)/2 \;+\; n_{virt}(n_{virt}+1)/2$. The rank of the linear system is however smaller than M, since projecting functions θ_{pq}^{+} are linearly dependent. It was pointed out[64] and can be checked based on Eq. (9), that a vector of zero norm is constructed as

$$\sum_i |\theta_{ii}^{+}\rangle \;-\; \sum_a |\theta_{aa}^{+}\rangle \;=\; 0\,. \tag{12}$$

As mentioned in Ref.,[64] the underdetermined PAPT equations define the zero-order apart from

a constant shift, which is immaterial from the point of view of PT. To look into this matter, let us rewrite Eq. (11) as

$$\sum_R T_{PR}\,\overline{F}_R \;=\; Y_P \tag{13}$$

where capital P is used as hyperindex for the generic index pair pq. To be more specific, the inhomogeneous term of Eq. (13) reads

$$Y_P \;=\; \langle\theta^+_{pq}|H_{\mathscr{N}}|\Psi^{(1)}\rangle \tag{14}$$

while the matrix of the linear system is given as

$$T_{PR} \;=\; \langle\theta^+_{pq}|\omega_R\rangle \tag{15}$$

where, assuming that hyperindex R is associated with rs, $|\omega_R\rangle$ is defined as

$$|\omega_R\rangle \;=\; \left(E^r_s - \langle E^r_s\rangle\right)|\Psi^{(1)}\rangle\,. \tag{16}$$

Let us invoke the singular value decomposition (SVD)[86,87] of T in the form

$$T \;=\; U\,\Sigma\,V^\dagger$$

with U and V unitary and the entries of the diagonal Σ being σ_P. Substituting the SVD form of T into Eq. (13), the PAPT equations are decoupled as

$$\sigma_P\,\overline{F}'_P \;=\; Y'_P\;, \qquad P=1,\ldots,M \tag{17}$$

where

$$\overline{F}'_P = \sum_R V_{RP}\,\overline{F}_R\,, \tag{18a}$$

$$Y'_P = \sum_R U_{RP}\,Y_R\,. \tag{18b}$$

As shown in the Appendix in detail, one singular value of T is zero, as a result of the the linear dependence of θ^+_{pq}. The corresponding left singular vector (column of U) describes the linear combination of θ^+_{pq} producing a vector of zero norm. Taking index M for which $\sigma_M = 0$, we have $U_{ii,M} = -U_{aa,M} = 1/\sqrt{n_{\text{basis}}}$ and $U_{pq,M} = 0$ for all $p \neq q$, c.f. Eq. (12). This means, that $Y'_M \sim \sum'_i Y_{ii} - \sum'_a Y_{aa} = 0$ and the $P = M$ case of Eq. (17) is satisfied irrespective of the value of $\overline{F}'_M$. In other words, a linear combination of parameters $\overline{F}_P$, described by the M'th right singular vector (column of V, c.f. Eq. (18b)) remains undetermined, due to the linear dependence of θ^+_{pq}.

In order to identify the M'th right singular vector, observe that functions ω_R are also linearly dependent, since

$$\sum_p |\omega_{pp}\rangle = \sum_p E^p_p |\Psi^{(1)}\rangle - \left(\sum_p \langle E^p_p\rangle\right)|\Psi^{(1)}\rangle = 0\,. \tag{19}$$

Relying on the Appendix, we can then see that the M'th right singular vector of T describes the linear combination of ω_R producing a vector of zero norm, i.e. $V_{pp,M} = 1/\sqrt{n_{\text{basis}}}$ and $V_{pq,M} = 0$ for all $p \neq q$. As a result, the combination of $\overline{F}_P$ not determined by the PAPT equations is found to be

$$\overline{F}'_M = \sum_p \overline{F}_{pp} = \mathrm{Tr}\overline{F}\,. \tag{20}$$

The above expression is exactly what we aimed for, since altering the trace of $\overline{F}$ represents a constant shift of the operator, that is administered at the zeroth and first term of the energy in a trivial manner and has no consequence at higher orders. It is for this formal proof that the SVD-based solution of Eq. (11) is needed. In practice, SVD of T can be circumvented by applying a

linear solver allowing for singular matrices.

Note that the above derivation hinges upon the use of the normal ordered form, $\overline{F}_{\mathscr{N}}$. Writing Eq. (11) with H and $\overline{F}$, instead of $H_{\mathscr{N}}$ and $\overline{F}_{\mathscr{N}}$, the M'th right singular vector of T is different from the above. The noninformative $P = M$ case of the decoupled set of equations leaves an $\overline{F}'_M$ undetermined which however contributes to the PT corrections. The PT terms get well defined once an extra equation is supplied. When taking $\langle\overline{F}\rangle = \langle H\rangle$ as the additional requirement, one gets back to Eq. (11).

On PAPT orbitals

Orbitals ψ_p, obtained from the set of canonical orbitals by transformation with the eigenvectors of $\overline{F}$ are termed PAPT orbitals. Spatial symmetry of PAPT orbitals follow from the structure of $\overline{F}$ arising as the solution of Eq. (13). It is relatively straightforward to see, that $\overline{F}$ exhibits a block-diagonal form, with nonzero $\overline{F}_{pq}$ occurring when φ_p and φ_q belong to the same irreducible representation (ir) of the molecular point group.

Let us first inspect Y_P of Eq. (14), with hyperindex P standing for pq. Since $H_{\mathscr{N}}|\Psi^{(1)}\rangle$ belongs to the totally symmetric ir, denoted by Γ_1, θ^+_{pq} should also transform according to Γ_1 to allow for a nonzero scalar product. Examining the first term on the right hand side of Eq. (9a), we focus on what nature of indices i and j ensure that θ^+_{ij} is totally symmetric. Since c^{ik}_{ab} is a coefficient of the totally symmetric $\Psi^{(1)}$, the ir of orbital i, Γ_i, matches the direct product of the ir of the other three orbitals, $\Gamma_a \otimes \Gamma_b \otimes \Gamma_k$. In order for the excited function $E^{ab}_{jk}|\mathrm{HF}\rangle$ to belong to Γ_1, it is now the ir of orbital j, Γ_j that should match the direct product $\Gamma_a \otimes \Gamma_b \otimes \Gamma_k$. The other terms of Eq. (9) are completely analogous, we can therefore conclude that $\Gamma_p = \Gamma_q$ should hold to allow for a nonzero Y_P.

Proceed now to matrix T, with elements given by Eq. (15) and focus on totally symmetric functions θ^+_{pq}, meaning $\Gamma_p = \Gamma_q$. For T_{PR} to be nonzero, ω_R should transform according to Γ_1, which, taking into account Eq. (16) is ensured by $\Gamma_r = \Gamma_s$. Establishing the symmetry of hyperindex P as $\Gamma_p \otimes \Gamma_q$ we see that matrix T couples hyperindices belonging to Γ_1 among themselves and this

property carries over for its inverse too. As a result, $\overline{F}_P$ obtained from Eq. (13) can be nonzero if P belongs to Γ_1, i.e. $\Gamma_p = \Gamma_q$.

Self-consistent PAPT

Corrections to the HF approximation by PAPT rest on the partitioning

$$H_{\mathscr{N}} = \overline{F}_{\mathscr{N}} + W_{\mathscr{N}} \tag{21}$$

with $\overline{F}_{\mathscr{N}}$ determined from Eq. (13). The first order correction to the HF energy is zero with the choice $\langle \overline{F} \rangle = \langle H \rangle$ while the first order correction to the HF determinant reads

$$\Psi^{(1)}_{\text{PAPT}} = \sum_{ijab} d^{ij}_{ab} \sum_{\sigma\sigma'} \psi^{\dagger}_{a\sigma} \psi^{-}_{i\sigma} \psi^{\dagger}_{b\sigma'} \psi^{-}_{j\sigma'} |\text{HF}\rangle \tag{22}$$

with d^{ij}_{ab} given as

$$d^{ij}_{ab} = -\frac{1}{2} \frac{\langle \psi_i \psi_j | \psi_a \psi_b \rangle}{\overline{\varepsilon}_a + \overline{\varepsilon}_b - \overline{\varepsilon}_i - \overline{\varepsilon}_j} \tag{23}$$

and $\psi_i, \overline{\varepsilon}_i$ introduced in Eq. (4). Concise form of low order PAPT energy corrections can be given with $\Psi^{(1)}_{\text{PAPT}}$ as

$$E^{(2)}_{\text{PAPT}} = \langle \text{HF} | H_{\mathscr{N}} | \Psi^{(1)}_{\text{PAPT}} \rangle \,, \tag{24a}$$

$$E^{(3)}_{\text{PAPT}} = \langle \Psi^{(1)}_{\text{PAPT}} | W_{\mathscr{N}} | \Psi^{(1)}_{\text{PAPT}} \rangle \,. \tag{24b}$$

The possibility of setting PAPT self-consistent is mentioned in Ref.,[64] meaning that once the PAPT zero-order is obtained based on the 1st order MP wavefunction, the first order PAPT wavefunction can be fed back to the PAPT equations generating a new zero-order. In formulae, wavefunction parameters Eq. (23) can be used to define projection functions Eq. (9), and Eq. (22) can be used to write Eq. (11) for the matrix elements of the zero-order. The procedure can be repeated till $\Psi^{(1)}_{\text{PAPT}}$

becomes consistent with $\overline{F}_{\mathscr{N}}$. Results obtained by this procedure are labeled PAPT-SC.

When iterated till self-consistency, the third order energy term of PAPT becomes zero. This property, shared with Feenberg scaling,[50] Adams partitioning[53] and other optimized partitionings[40,54] can be shown in formulae by e.g. arranging the self-consistent version of Eq. (11a) as

$$\langle \theta_{ij}^{+} | H_{\mathscr{N}} - \overline{F}_{\mathscr{N}} | \Psi_{\mathrm{PAPT}}^{(1)} \rangle \;=\; 0\,,$$

and summing the $i = j$ terms, multiplied by 0.5

$$\frac{1}{2}\sum_{i} \langle \theta_{ii}^{+} | H_{\mathscr{N}} - \overline{F}_{\mathscr{N}} | \Psi_{\mathrm{PAPT}}^{(1)} \rangle \;=\; 0\,.$$

Observing that $\Psi_{\mathrm{PAPT}}^{(1)} = \frac{1}{2}\sum_i \theta_{ii}^{+}$ once coefficients of Eq. (23) are used in Eq. (9) and taking into account Eq. (21), the left hand side of the above expression is the self-consistent PAPT energy at order three.

Once self-consistency of PAPT is achieved, Feenberg scaling[50] is not any more effective. This is most easily seen by noting that Feenberg scaling, which means a repartitioning of the Hamiltonian as

$$H \;=\; \underbrace{\frac{1}{1-\mu}\,H^{(0)}}_{H^{(0)\prime}} \;+\; \underbrace{W \;+\; \frac{\mu}{1-\mu}\,H^{(0)}}_{W'}$$

with the scaling parameter μ fixed by making the new third order energy zero, yields a new second-order energy that can be recast to the form[50,88]

$$E^{(2)\prime} \;=\; \frac{(E^{(2)})^2}{E^{(2)} - E^{(3)}}.$$

It is then clear that if, in any partitioning, one has $E^{(3)} = 0$, then $E^{(2)\prime} = E^{(2)}$, i.e., the original and Feenberg's second order energies coincide.

Applications

Assessment of PAPT results collected in this Section is aided by comparison to optimalization strategies addressing level-shifts only. One of the latter the methods, termed OPT-LS below, fixes the value of $\overline{F}_{pp}$ in Eq. (5) by requiring that the PT energy summed up to order three is stationary with respect to infinitesimal variation of these parameters.[81] Optimizing PT denominators of doubly excited determinants of the Hilbert-space in the same spirit leads to the linearized coupled-cluster doubles (LCCD) model.[40] Note, that the number of parameters optimized is markedly different in the two approaches, $n_{basis} - 1$ and $n_{occ}^2 n_{virt}^2$ in OPT-LS and LCCD, respectively. Though OPT-LS is more akin to PAPT-LS regarding the parameter space, the main role of both OPT-LS and LCCSD results shown below is to provide a basis of comparison for PAPT-LS. Benchmarking of all PT methods is assisted by Full-CI whenever computationally attainable. In lack of this, CCSD and CCSD(T) are shown for benchmark in weak correlation scenarios.

Total energies

The potential energy curves for the H_2 molecule in cc-pVTZ basis[89] calculated by HF, traditional MP and standard PAPT are displayed in Figure 1 with Full-CI serving as reference. Fig. 1(b) depicts polynomial curves of degree eight fitted around equilibrium bond distance. Of second and third order of PAPT, only PAPT3 is displayed in Fig. 1(b) as they could not be discerned on the scale of the plot. As Fig. 1 reflects, the approximation of the potential curve improves in the order of MP2, MP3 and PAPT. The latter run closer to Full-CI at around equilibrium and start to deviate at a larger bond length than MP2 or MP3. Although it slightly overestimates the correlation energy, the shape of the PAPT3 curve around equilibrium is apparently superior to MP3. Equilibrium bond lengths and quadratic force constants deduced from the polynomial fit, collected in Table 1, complement the picture. Table 1 shows that the error (with respect to Full-CI) of PAPT2 and PAPT3 is approximately -0.03% and 0.06% respectively, for the bond length and 0.3% and -0.3% respectively, for the force constant. In comparison, the error of MP3 is cca. -0.4%

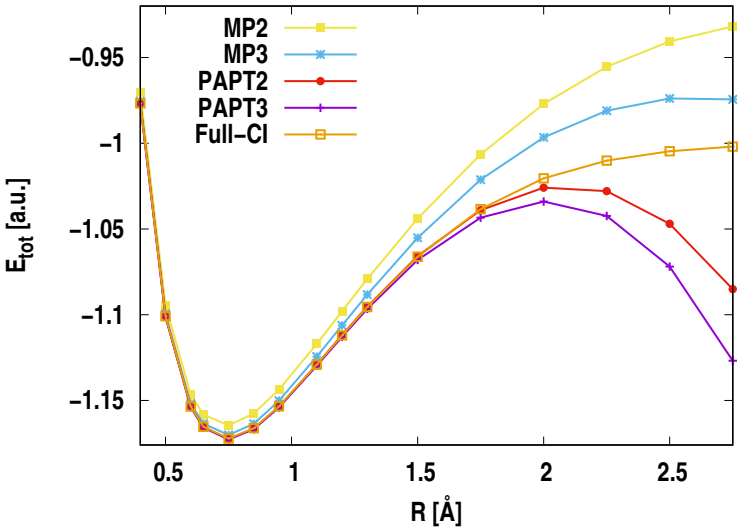

(a)

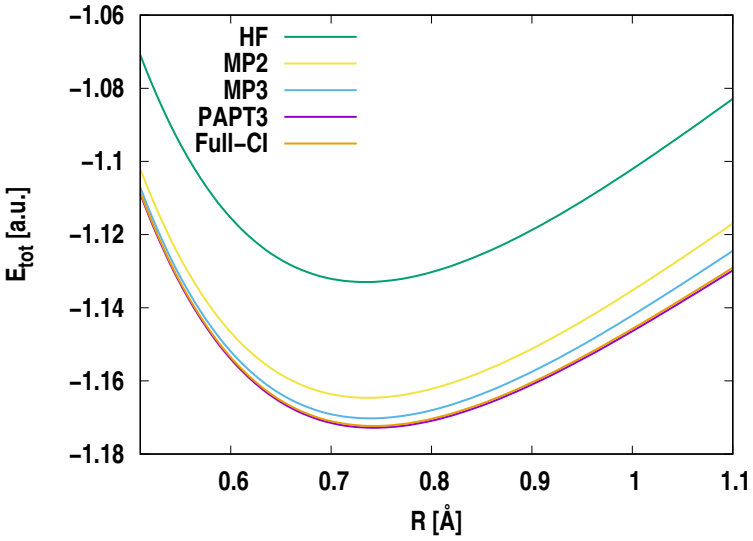

(b)

Figure 1: Potential energy curve of the H_2 molecule in cc-pVTZ basis taken with HF, MP, PAPT and Full-CI. Panel (b) is a zoom into the minimum region of the wider bond distance plot in panel (a).

for the bond length and 3% for the force constant.

A more challenging example is provided by the distortion of the linear BeH_2 molecule into a singlet coupled system of three separated atoms. At the geometry points A-I, set by Purvis and Bartlett[92] the Be atom lays in the origin and the two H atoms are placed symmetrically to the z-axis with coordinates in atomic unit $(0, \pm 2.54, 0)$, $(0, \pm 2.08, 1.0)$,

Table 1: Equilibrium bond lengths (r) and quadratic force constants (K) of the H_2 molecule from polynomial curves of degree 8 fitted in the bond distance interval [0.5,1.25] Å.

	Bond length r **[Å]**	**Force constant** K **[a.u.]**
HF	0.7340	0.3997
MP2	0.7366	0.3889
MP3	0.7391	0.3801
PAPT2	0.7420	0.3697
PAPT3	0.7426	0.3676
Full-CI	0.7422	0.3686
Experimental[90,91]	0.7414	0.3680

$(0,\pm1.62,2.0)$, $(0,\pm1.39,2.5)$, $(0,\pm1.275,2.75)$, $(0,\pm1.16,3.0)$, $(0,\pm0.93,3.5)$, $(0,\pm0.70,4.0)$, and $(0,\pm0.70,6.0)$, respectively. Starting from a situation dominated by a closed shell determinant at point A, the single reference approach gradually breaks down as the distortion takes place. Points E and F are especially challenging for two determinants becoming of comparable weight in the Full-CI solution.

Table 2: Total energies of BeH_2 in cc-pVTZ basis taken with HF, MP3, PAPT3, PAPT3-SC, CCSD and FCI as reference.

codified geometries	HF E_{tot} [a.u.]	Full-CI E_{tot} [a.u.]	MP3 E_{tot} [a.u.]	PAPT3 E_{tot} [a.u.]	PAPT3-SC E_{tot} [a.u.]	CCSD E_{tot} [a.u.]
A	-15.77138	-15.85679	-15.85210	-15.85726	-15.85741	-15.85588
B	-15.73892	-15.82759	-15.82307	-15.82805	-15.82818	-15.82663
C	-15.66635	-15.76102	-15.75506	-15.76109	-15.76133	-15.75955
D	-15.60384	-15.70531	-15.69639	-15.70392	-15.70478	-15.70295
E	-15.56761	-15.67808	-15.66277	-15.67209	-15.67786	-15.67301
F	-15.53187	-15.68325	-15.62970	-15.64743	not. conv.	-15.66265
G	-15.63703	-15.74069	-15.72748	-15.74219	-15.74463	-15.73858
H	-15.68140	-15.77790	-15.76687	-15.78004	-15.78197	-15.77657
I	-15.70335	-15.79496	-15.78450	-15.79772	-15.79958	-15.79450

Fig. 2 assists to judge the quality of the total energies of the system collected in Table 2. As apparent in Fig. 2, difference from Full-CI by CCSD lies on the order of a couple of mHa but grows to the 20 mHa regime at point F, reflecting the inherent problem of the single determinant based approach. While this phenomenon can not be expected to be cured by HF based PAPT, it is interesting to observe its performance at the less troublesome but still challenging points.

Comparison to MP3 shows that a considerable improvement is brought about by PAPT3 along the entire process, omitting point F. The 5-15 mHa error of MP3 is cut back to the 1 mHa range in absolute value by PAPT3 at points A-E and a somewhat larger but still improved error regime of 5 mHa in absolute value is attained at geometry points G-I by PAPT3. Performance of the self-consistent version of PAPT is more diverse than PAPT3. While the effect of PAPT3-SC is negligible at points A-C, its improvement over PAPT3 is impressive at points D-E but deteriorates PAPT3 errors by a rough factor of two at points G-I. At the genuinely multireference point F, the self-consistent iteration did not converge by successive PAPT calculations. (Damping procedures were not applied.) This indicates that the self-consistent PAPT variant may need more prudence than PAPT itself when applied in the presence of static correlation.

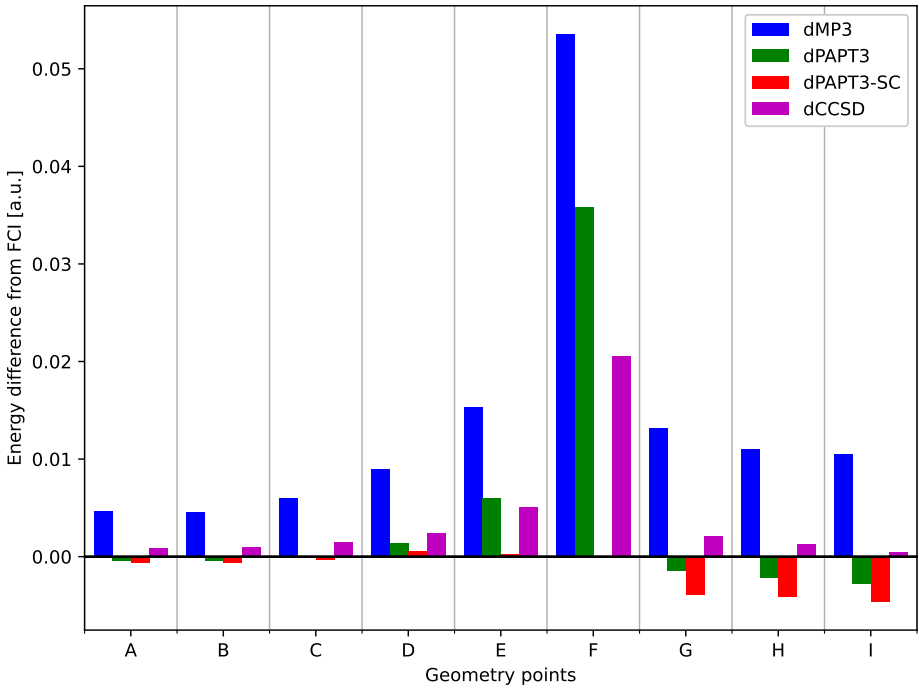

Figure 2: Energy differences (ΔE) in millihartree of MP3, PAPT3, PAPT3-SC and CCSD from the FCI reference for geometries A-I of BeH_2 using the data presented in Table 2.

Conformation energy barriers

Partitioning variants based on PAPT are contested with MP, OPT-LS and LCCSD on the example of energy barriers for theoretical conformation changes of H_2O, NH_3 and CH_4. Geometries are optimized at the HF level in 6-311G** basis[93] at C_{2v} and $D_{\infty h}$ symmetry arrangements of H_2O, C_{3v} and D_{3h} arrangements of NH_3 and a C_{3v} and T_d conformations of CH_4. Single point energies behind the barriers collected in Table 3 are calculated in cc-pVTZ basis at the optimized geometries. Benchmark is provided by CCSD(T) in Table 3, for comparison CCSD is also included.

Table 3: Energy barriers taken with HF, MP, various PAPT and CC methods for linear and bent H_2O, planar and pyramidal NH_3, C_{3v} and tetrahedral CH_4 molecular conformations respectively.

	H_2O	**NH_3**	**CH_4**
	ΔE [mE_h]		
HF	52.78	8.55	39.92
MP2	52.21	8.83	34.35
MP3	52.72	8.97	34.79
OPT2-LS	52.65	8.83	34.93
OPT3-LS	52.60	8.83	34.93
LCCSD	53.46	9.48	34.42
PAPT2	52.88	9.08	34.88
PAPT3	52.92	9.11	34.87
PAPT2-LS	53.15	9.18	34.57
PAPT3-LS	52.88	8.95	34.84
PAPT2-ROT	52.26	9.37	34.41
PAPT3-ROT	53.01	9.10	34.80
PAPT2-SC	52.94	9.13	34.86
PAPT3-SC	52.94	9.13	34.86
CCSD	53.10	9.18	35.07
CCSD(T)	53.29	9.43	34.42

We start by observing that PAPT3 improves over the MP3 barriers of H_2O and NH_3, reducing the error by some 25-30%. The case of CH_4 shows an opposite effect, the error of PAPT3 being worse than that of MP3 by cca. 25%. For all three systems in Table 3, PAPT3 is either better or essentially of the same quality as PAPT2.

Inspecting PAPT-LS, OPT-LS and LCCSD results in Table 3 we can get an impression of the performance of simple level-shift techniques vis-à-vis the more sophisticated PAPT approach.

One can resort to the level-shift component of PAPT, whereby PAPT2-LS yields better barriers than PAPT3, while PAPT3-LS barriers are of MP3 quality only. The level-shift optimalization method, OPT-LS is manifestly inferior to PAPT3 and deteriorate with stepping from second to third order. While PAPT2-LS appears to give ground for praise of the level-shift methodology, the initial enthusiasm is dampened by two factors. First, total energies by PAPT2-LS are systematically the largest among all tabulated methods. (E.g. the error in correlation energy is cca. 2.5% by PAPT2 and PAPT3 for both conformers of H_2O while the same is 6.8% by PAPT2-LS.) Second, the PAPT-LS results worsen instead of improving as the order of PT increases. Based on this, PAPT-LS appears a less reliable approach than the full blown version of PAPT in spite of fact that conformational PAPT2-LS barriers appear competitive with PAPT. It is interesting to observe in Table 3, that while PAPT essentially brings CCSD quality results, the level-shift related LCCSD values are even better, providing the closest values to the CCSD(T) benchmark for all three systems.

Stepping to the orbital rotation component, PAPT-ROT barriers are occasionally better than full PAPT, but the improvement is again not systematic with the order of PT. For NH_3 and CH_4 it is PAPT2-ROT that significantly reduces the error of the PAPT3 barrier, while it is PAPT3-ROT that outperforms PAPT3 for H_2O. Since PAPT-ROT can be considered a PAPT orbitals-based Kapuy-partitioning, juxtaposing PAPT2-ROT with MP2 is particularly interesting and somewhat unexpectedly shows that the numerical results for the barriers are better by Kapuy's approach than by MP2. The picture is the same, when considering total energies.

Self-consistent solution of the PAPT equations bring a rather marginal change in the barrier, an order of magnitude smaller than the deviation of PAPT3 from CCSD(T). Note, that PAPT3-SC is the same as PAPT2-SC in agreement with the Section where the self-consistent version of PAPT is discussed.

PAPT orbitals

A glimpse on Fig. 3 helps to get an impression of the orbital transformation implied by PAPT. The example is provided by the C_{2v} geometry of H_2O, taking the three dimensional totally symmetric block of the occupied block of $\overline{F}$. Isocontours are drawn at two values for all three cases, i.e. the $1a_1$, $2a_1$ and $3a_1$ occupied MOs. According to Fig. 3 the node structure of PAPT MOs is somewhat enhanced as compared to canonical MOs but altogether the effect is relatively small (note the isocontour values in the column DIFF). In particular, the $1a_1$ core MO, that is essentially a 1s atomic orbital on oxygen, gets significantly delocalized over the hydrogen atoms by PAPT.

Dispersion interaction energies

Dispersive van der Waals interaction is studied on the example of a He dimer, computed in aug-cc-pVTZ basis using Boys-Bernardi counterpoise correction.[94] Interaction energy as a function of interatomic distance, plotted in Fig. 4 shows, that though both MP3 and PAPT3 lie close to Full-CI, MP3 is closer. Comparing the $\mathscr{O}(6)$ scaling schemes of MP3, CCSD and PAPT3 in Fig. 4, performance of the latter obviously falls behind the former two. The room for improvement apparent in Fig. 4 from CCSD to Full-CI is nicely covered when triple excitations are brought into play by the $\mathscr{O}(7)$ scaling noniterative correction of CCSD(T). Total energies, collected in Table 4 provide some insight into the microHartree level inadequacy of PAPT3 in this example. While PAPT3 is consistently superior to MP3 as indicated by the figures in Table 4, deviation from Full-CI is more imbalanced by PAPT3 than with MP3.

Convergence of self-consistent PAPT calculations

As discussed above, the Knowles equations can be solved iteratively until self-consistency is achieved. A short study on the convergence features of this iteration is carried out on the example of the HF molecule at various H–F bond lengths and in various basis sets.

Table 5 presents second order energies for equilibrium, medium and prolongated H–F distances

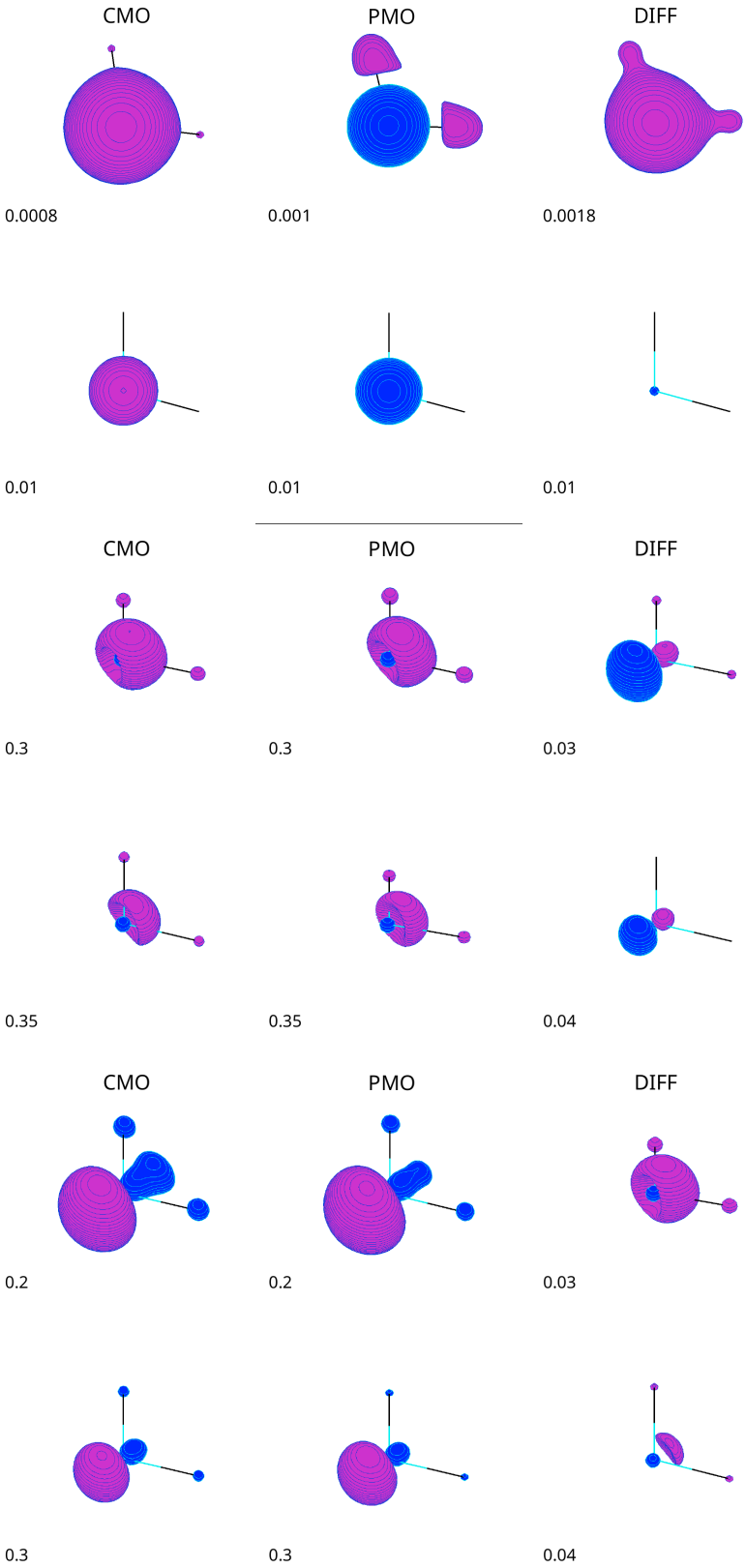

Figure 3: Visualization of canonical and PAPT MOs and their difference for the $1a_1$ (top) $2a_1$ (middle) and $3a_1$ (bottom) occupied orbitals of bent H_2O molecule at different space contours to illustrate the sterical properties.

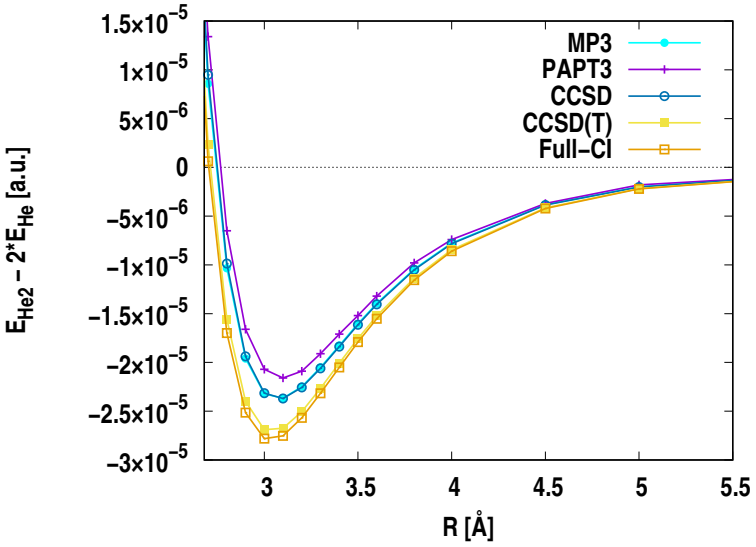

Figure 4: Difference between total energies of He_2 and two helium atoms in aug-cc-pVTZ basis taken with MP3, PAPT3, CCSD, CCSD(T) and Full-CI.

Table 4: Correlation energies of a He dimer and a monomer (computed in the dimer basis) at various interatomic distances (R) taken with MP3, PAPT3 and Full-CI as reference in aug-cc-pVTZ basis set.

System	**Distance**	**MP3**	**PAPT3**	**FCI**
	R **[Å]**	$E_{\mathbf{corr}}$ **[mE$_h$]**		
He	2.8	-38.446	-39.696	-39.417
	3.0	-38.445	-39.695	-39.416
	3.2	-38.445	-39.695	-39.416
He_2	2.8	-76.964	-79.460	-78.912
	3.0	-76.938	-79.436	-78.884
	3.2	-76.922	-79.420	-78.867

as functions of the number of iteration steps. It shows that the convergence (without applying any acceleration techniques) is quite fast: at around equilibrium requiring merely 5 and at double equilibrium distance only 15 iterations to achieve μH accuracy, but even for 2.5 R_e the second order energy has converged to some 10 μH accuracy in 25 steps.

We note that, while one clearly expects poor convergence or even divergence of a single-reference PTn series at large distances, it is not a priori evident why the PAPT iteration becomes slower for prolongated bond lengths. However, we did not see divergent PAPT iterations for this system (unlike for point F of BeH_2 in Table 2).

Table 6 presents second and third order PAPT contributions in three different basis sets with increasing flexibility for the HF molecule at around equilibrium bond length. The third order contributions, which should tend to zero upon convergence, are shown as indicators. Self-consistency of PAPT is reached within 4–5 iterations in each basis set, but it is interesting to observe that most PAPT3 contributions are significantly smaller in the larger bases even at the first and second iteration steps. From the third step on, the results do not exhibit any notable differences.

Table 5: Convergence of the second order cc-pVDZ energies (in Hartrees) during the iteration in self-consistent PAPT for the HF molecule at equilibrium R_e = 0.901461 Å, 2.0 R_e and 2.5 R_e bond lengths.

no. of iterations	R_e	2.0 R_e	2.5 R_e
1	-0.206569	-0.248386	-0.286706
2	-0.206692	-0.252349	-0.298242
10	-0.206707	-0.255372	-0.307393
15	-0.206707	-0.255383	-0.307471
20	-0.206707	-0.255383	-0.307493
25	-0.206707	-0.255383	-0.307502

Conclusion

An analysis of the Knowles partitioning with the help of the established concepts of energy level-shifts and orbital rotation has been provided. Level-shift component, PAPT-LS is identified in the

Table 6: Basis set dependence of the convergence of self-consistent PAPT iterations for the HF molecule at equilibrium geometry (R_e = 0.901461 Å). The 2nd and 3rd order PAPT contributions are shown in Hartrees.

	PAPT2			PAPT3		
no. of iterations	cc-pVDZ	cc-pVTZ	aug-cc-pVTZ	cc-pVDZ	cc-pVTZ	aug-cc-pVTZ
1	-0.206569	-0.285675	-0.293603	-0.000113	-0.000036	-0.000055
2	-0.206692	-0.285724	-0.293674	-0.000011	-0.000006	-0.000002
3	-0.206703	-0.285731	-0.293677	-0.000003	-0.000004	-0.000003
4	-0.206706	-0.285735	-0.293681	-0.000001	-0.000001	-0.000001
5	-0.206707	-0.285736	-0.293682	0.000000	0.000000	0.000000

canonical molecular orbital basis in a straightforward manner. The effect of orbital rotation solely, denoted PAPT-ROT is grasped by formulating a Kapuy-type zero-order Hamiltonian on the basis of PAPT orbitals. The two effects are not additive. Getting to PAPT from PAPT-ROT requires fixing the energy levels of *PAPT orbitals*. From this standpoint, Knowles' partitioning can be interpreted as a level-shifted Kapuy-partitioning and its success can be attributed to the particular choice of orbitals and orbital energies.

Orbitals behind PAPT are nonlocal, exhibiting spatial symmetry of the system. Deviation from canonical HF orbitals is seemingly rather minor, the node structure getting slightly enhanced. At difference with Kapuy-partitioning built on localized HF orbitals, delocalized PAPT orbitals based Kapuy-partitioning provides an example for outperforming MP.

Compared to previously suggested level-shift optimalization in Fock-space,[81] PAPT-LS is found superior. The performance of separate level-shift or orbital rotation contribution of PAPT is occasionally good but can not be claimed reliable, the picture changing with system, or with stepping from total energies to energy differences. Neither of the two components are dominating over the other. Level-shift and orbital rotation are roughly equal contributors in PAPT, and work in synergy to achieve a systematic improvement over MP results.

A set of examples, involving systems affected by weak and strong correlation shows PAPT to be of CCSD quality. Examples where PAPT3 is inferior to MP3 are rare. One such case is the He dimer, where total energies of the monomer and dimer are well behaving, a slight imbalance however results in the counterpoise corrected interaction energy being reproduced better by MP3

than by PAPT, on the order of μE_h. Self-consistent iteration of PAPT invariably improves the results in single determinant dominated situations and requires a couple of iterations, the number of steps found fairly independent on basis set size.

The success of PAPT corrections emphasizes that an appropriate set of HF molecular orbitals, different from canonicals, and an appropriate set of orbital energies, different from Koopmans' values can be a better choice than the generally used MP partitioning.

Acknowledgments

The authors are thoroughly indebted to Prof. Peter Knowles (Cardiff, UK), for extensive discussions on the subject and for sharing some of his results for comparisons to test our code.

Appendix

Davidson's A-matrix

Suppose that a one-electron operator is given in the form

$$\overline{F} \;=\; \sum_{pq} \overline{F}_{pq}\, E^p_q$$

where p,q are spatial indices of generic HF molecular orbitals and $\overline{F}$ complies with the Brillouin-theorem in that $\overline{F}_{ia} = \overline{F}_{ai} = 0$ for i occupied and a virtual. Consider also the Hamiltonian, written using the same set of orbitals as

$$H \;=\; \sum_{pq} h_{pq}\, E^p_q \;+\; \frac{1}{2} \sum_{pqrs} \langle pq|rs\rangle \left(E^p_r E^q_s - \delta_{qr} E^p_s \right) . \qquad (25)$$

Based on the results of Davidson[68] it is possible to rewrite the Hamiltonian with modified integrals $\overline{h}_{pq}$ and $\overline{\langle pq|rs\rangle}$ in the form

$$H = \sum_{pq} \overline{h}_{pq} E^p_q + \frac{1}{2} \sum_{pqrs} \overline{\langle pq|rs\rangle} \left(E^p_r E^q_s - \delta_{qr} E^p_s \right) , \tag{26}$$

where the significance of integrals with overbar is that they build the elements of $\overline{F}$ as usual for a Fockian, i.e.

$$\overline{F}_{pq} = \overline{h}_{pq} + \sum_j^{\text{occ}} \left(2\overline{\langle pj|qj\rangle} - \overline{\langle pj|jq\rangle} \right) . \tag{27}$$

Note however, that $\overline{F}$ differs from the Fockian, the elements of the latter given by

$$F_{pq} = h_{pq} + \sum_j^{\text{occ}} (2\langle pj|qj\rangle - \langle pj|jq\rangle) . \tag{28}$$

Integrals $\overline{h}_{pq}$ and $\overline{\langle pq|rs\rangle}$ are derived by Davidson with the help of a Hermitian one-body operator

$$A = \sum_{pq} A_{pq} E^p_q$$

that is added and subtracted to H of Eq. (25) to yield[68,82]

$$\overline{h}_{pq} = h_{pq} + A_{pq} \tag{29a}$$

$$\overline{\langle pq|rs\rangle} = \langle pq|rs\rangle - \frac{A_{pr}\delta_{qs} + A_{qs}\delta_{pr}}{N-1} \tag{29b}$$

where N denotes the number of electrons in the system. With the use of Eqs.(27)-(28) and Eq. (29), the unique relation between elements A_{pq} and $\overline{F}_{pq}$ can be found as[85]

$$\overline{F}_{pq} - F_{pq} = A_{pq} \left(1 - \frac{N}{N-1} + \frac{n_p + n_q}{N-1} \right) - \frac{2\delta_{pq}}{N-1} \text{Tr}_o A \tag{30}$$

where $\text{Tr}_o A = \sum_i^{occ} A_{ii}$ and n_p taking values 0 or 1 for p virtual or occupied, respectively.

Given an $\overline{F}$ different from F, a set of molecular orbitals diagonalizing $\overline{F}$ are termed 'proper canonicals' by Davidson. When working with noncanonical (c.f. F is nondiagonal) but proper canonical orbitals, the form of Eq. (26) of the Hamiltonian has the advantage, that matrix elements in between determinants related by a single excitation yield elements of $\overline{F}$ that is proportional to Kronecker-delta. In this sense proper canonical orbitals show some features of canonicals when used in conjunction with Eq. (26). Obtaining integrals with overbar proceeds via Eq. (29).

Approaching from the angle where a set of noncanonical orbitals is provided, one may aim for constructing a diagonal $\overline{F}$ to which the given orbitals a proper canonicals. Based on Eq. (30), $\overline{F}_{pq} = 0$ for $p \neq q$ fixes the nondiagonal elements of A but leaves A_{pp} arbitrary. Generating the integrals with overbar with either of such A-matrices according to Eq. (29) allows to make use of the diagonality of $\overline{F}$ when computing matrix elements of H. This technique, referred to as integral dressing,[85] facilitates to obtain PT corrections with a canonical many-body PT implementation, in noncanonical, e.g. PAPT orbitals, applying either Kapuy's or PAPT zero-order. In the former case $A_{pp} = 0$ is applied while in the latter A_{pp} is set from Eq. (30) so that $\overline{F}_{pp}$ matches PAPT orbital energies.

Redundancy in pairing

Starting from Eq. (15), with somewhat simplified notation, consider an $M \times M$ matrix T given by the elements

$$T_{PR} = \langle \theta_P | \omega_R \rangle \, .$$

The SVD[86,87] of T written as

$$T = U \Sigma V^{\dagger} \tag{31}$$

solves the pairing problem, i.e. it provides a set of vectors θ'_P and ω'_R fulfilling

$$\langle \theta'_P | \omega'_R \rangle \;=\; \delta_{PR}\sigma_P$$

where σ_P are the diagonal entries of the singular value matrix Σ, and the paired vectors arise as

$$\langle \theta'_P | \;=\; \sum_Q (U^\dagger)_{PQ} \langle \theta_Q | \,, \tag{32a}$$

$$| \omega'_R \rangle \;=\; \sum_Q | \omega_Q \rangle V_{QR} \,. \tag{32b}$$

Consider now the case where the overlap of vectors θ_P

$$S_{PR} \;=\; \langle \theta_P | \theta_R \rangle$$

is singular, in particular let us suppose that the eigenvalue problem of S written as

$$W^\dagger S W \;=\; s^{diag}$$

produces $s_M = 0$ and $s_P \neq 0$ for $P = 1, \ldots, M-1$, residing in the diagonal of s^{diag}. This means that the set of θ_P is linearly dependent and among vectors

$$\langle \tilde{\theta}_P | \;=\; \sum_Q (W^\dagger)_{PQ} \langle \theta_Q | \tag{33}$$

that corresponding to $P = M$ is of zero norm

$$\langle \tilde{\theta}_M | \tilde{\theta}_M \rangle \;=\; (W^\dagger S W)_{MM} \;=\; s_M \;=\; 0 \,,$$

c.f. Eq. (12). We wish to show that for index M

$$\langle \tilde{\theta}_M | \;=\; \langle \theta'_M |$$

holds with $\sigma_M = 0$, i.e. the zero norm vector constructible with θ_P is an element of the paired set and corresponds to a zero singular value.

For this end let us consider $\tilde{T}$ built with

$$\tilde{T}_{PR} \;=\; (W^\dagger T)_{PR} \;=\; \langle \tilde{\theta}_P | \omega_R \rangle$$

and generate its left singular vectors as eigenvectors of $\tilde{T}\tilde{T}^\dagger$. The M'th row and column of the latter matrix is obviously zero since

$$(\tilde{T}\tilde{T}^\dagger)_{PR} \;=\; \langle \tilde{\theta}_P \sum_Q |\omega_Q\rangle\langle\omega_Q|\, \tilde{\theta}_R \rangle$$

and $\tilde{\theta}_M$ is a vector of zero norm. The $M \times M$ matrix $\tilde{U}$ collecting the eigenvectors of $\tilde{T}\tilde{T}^\dagger$ is consequently block-diagonal, taking the form

$$\tilde{U}^{M\times M} \;=\; \begin{pmatrix} \tilde{U}^{(M-1)\times(M-1)} & 0 \\ 0 & 1 \end{pmatrix} \tag{34}$$

and the M'th eigenvalue of $\tilde{T}\tilde{T}^\dagger$ is zero. Right singular vectors of $\tilde{T}$ agree with those of T, since $\tilde{T}^\dagger\tilde{T} \;=\; T^\dagger T$. This allows to write the SVD of $\tilde{T}$ as

$$\tilde{T} \;=\; \tilde{U}\tilde{\Sigma}V^\dagger$$

and deduce that the M'th entry of the diagonal matrix $\tilde{\Sigma}$ is $\tilde{\sigma}_M = 0$. The SVD of matrix T arises by transforming the above from the left by W leading to

$$T \;=\; W\tilde{U}\tilde{\Sigma}V^\dagger\,. \tag{35}$$

Comparing Eqs.(35) and (31), $U = W\tilde{U}$ and $\Sigma = \tilde{\Sigma}$ can be inferred and $\sigma_M = \tilde{\sigma}_M = 0$ follows from

the latter. The M'th element of the paired set is obtained by substituting into Eq. (32a) to get

$$\langle\theta'_M| \;=\; \sum_Q (\tilde{U}^\dagger W^\dagger)_{MQ}\,\langle\theta_Q| \;=\; \sum_Q (\tilde{U}^\dagger)_{MQ}\langle\tilde{\theta}_Q| \tag{36}$$

with the help of Eq. (33). Taking into account the structure of $\tilde{U}$ exhibited in Eq. (34), $\langle\tilde{\theta}_M|$ is recovered on the right hand side of Eq. (36). This completes the proof. The case of linear dependence affecting ω_R is completely analogous. When both θ_P and ω_R form redundant sets, the zero norm vectors are paired, with the corresponding singular value being zero.

References

(1) Møller, C.; Plesset, M. Note on an Approximation Treatment for Many-Electron Systems. *Phys. Rev.* **1934**, *46*, 618.

(2) Cremer, D. Møller–Plesset perturbation theory: from small molecule methods to methods for thousands of atoms. *Wiley Interdiscip. Rev. Comput. Mol. Sci.* **2011**, *1*, 509–530.

(3) Hirata, S.; He, X.; Hermes, M. R.; Willow, S. Y. Second-Order Many-Body Perturbation Theory: An Eternal Frontier. *J. Phys. Chem. A* **2014**, *118*, 655–672.

(4) Curtiss, L. A.; Raghavachari, K.; Redfern, P. C.; Rassolov, V.; Pople, J. A. Gaussian-3 (G3) theory for molecules containing first and second-row atoms. *J. Chem. Phys.* **1998**, *109*, 7764–7776.

(5) Goerigk, L.; Grimme, S. Double-hybrid density functionals. *Wiley Interdiscip. Rev. Comput. Mol. Sci.* **2014**, *4*, 576–600.

(6) Rolik, Z.; Kállay, M. A general-order local coupled-cluster method based on the cluster-in-molecule approach. *J. Chem. Phys.* **2011**, *135*, 104111.

(7) Nagy, P. R.; Samu, G.; Kállay, M. Optimization of the Linear-Scaling Local Natural Orbital CCSD(T) Method: Improved Algorithm and Benchmark Applications. *J. Chem. Theory Comput.* **2018**, *14*, 4193–4215.

(8) Pulay, P.; Saebø, S. Orbital-invariant formulation and second-order gradient evaluation in Møller-Plesset perturbation theory. *Theor. Chim. Acta* **1986**, *69*, 357.

(9) Saebø , S.; Pulay, P. Fourth-order Møller–Plessett perturbation theory in the local correlation treatment. I. Method. *J. Chem. Phys.* **1987**, *86*, 914.

(10) Almlöf, J. Elimination of energy denominators in Møller—Plesset perturbation theory by a Laplace transform approach. *Chem. Phys. Letters* **1991**, *176*, 319.

(11) Häser, M.; Almlöf, J. Laplace transform techniques in Møller–Plesset perturbation theory. *J. Chem. Phys.* **1992**, *96*, 489–494.

(12) Martinez, T. J.; Carter, E. A. Pseudospectral Møller–Plesset perturbation theory through third order. *J. Chem. Phys.* **1994**, *100*, 3631–3638.

(13) Maslen, P. E.; Head-Gordon, M. Non-iterative local second order Møller–Plesset theory. *Chem. Phys. Letters* **1998**, *283*, 102–108.

(14) Hetzer, G.; Pulay, P.; Werner, H.-J. Multipole approximation of distant pair energies in local MP2 calculations. *Chem. Phys. Letters* **1998**, *290*, 143–149.

(15) Hetzer, G.; Schütz, M.; Stoll, H.; Werner, H.-J. Low-order scaling local correlation methods II: Splitting the Coulomb operator in linear scaling local second-order Møller–Plesset perturbation theory. *J. Chem. Phys.* **2000**, *113*, 9443.

(16) Werner, H.-J.; Manby, F. R.; Knowles, P. J. Fast linear scaling second-order Møller-Plesset perturbation theory (MP2) using local and density fitting approximations. *J. Chem. Phys.* **2003**, *118*, 8149–8160.

(17) Surján, P. R. The MP2 energy as a functional of the Hartree–Fock density matrix. *Chem. Phys. Letters* **2005**, *406*, 318–320.

(18) Kobayashi, M.; Akama, T.; Nakai, H. Second-order Møller-Plesset perturbation energy obtained from divide-and-conquer Hartree-Fock density matrix. *J. Chem. Phys.* **2006**, *125*, 204106.

(19) Weijo, V.; Manninen, P.; Jørgensen, P.; Christiansen, O.; Olsen, J. General biorthogonal projected bases as applied to second-order Møller-Plesset perturbation theory. *J. Chem. Phys.* **2007**, *127*.

(20) Zienau, J.; Clin, L.; Doser, B.; Ochsenfeld, C. Cholesky-decomposed densities in Laplace-based second-order Møller–Plesset perturbation theory. *J. Chem. Phys.* **2009**, *130*, 204112.

(21) Willow, S. Y.; Kim, K. S.; Hirata, S. Stochastic evaluation of second-order many-body perturbation energies. *J. Chem. Phys.* **2012**, *137*, 204122.

(22) Barca, G. M. J.; McKenzie, S. C.; Bloomfield, N. J.; Gilbert, A. T. B.; Gill, P. M. W. Q-MP2-OS: Møller–Plesset Correlation Energy by Quadrature. *J. Chem. Theory Comput.* **2020**, *16*, 1568–1577.

(23) Förster, A.; Franchini, M.; van Lenthe, E.; Visscher, L. A Quadratic Pair Atomic Resolution of the Identity Based SOS-AO-MP2 Algorithm Using Slater Type Orbitals. *J. Chem. Theory Comput.* **2020**, *16*, 875–891.

(24) Bartlett, R. J.; III, G. D. P. Molecular Applications of Coupled Cluster and Many-Body Perturbation Methods. *Physica Scripta* **1980**, *21*, 255.

(25) Handy, N. C.; Knowles, P. J.; Somasundram, K. On the convergence of the Møller-Plesset perturbation series. *Theor. Chim. Acta* **1985**, *68*, 87.

(26) Christiansen, O.; Olsen, J.; Malmquist, P.-A. On the inherent divergence in the Møller-Plesset series. The neon atom – A test case. *Chem. Phys. Letters* **1996**, *261*, 369.

(27) Olsen, J.; Christiansen, O.; Koch, H.; Jørgensen, P. Surprising cases of divergent behavior in Møller–Plesset perturbation theory. *J. Chem. Phys.* **1996**, *105*, 5082–5090.

(28) Leininger, M. L.; Allen, W. D.; Schaefer, H. F.; Sherrill, C. D. Is Møller–Plesset perturbation theory a convergent ab initio method? *J. Chem. Phys.* **2000**, *112*, 9213–9222.

(29) Sergeev, A. V.; Goodson, D. Z.; Wheeler, S. E.; Allen, W. D. On the nature of the Møller-Plesset critical point. *J. Chem. Phys.* **2005**, *123*.

(30) Olsen, J.; Jørgensen, P.; Helgaker, T.; Christiansen, O. Divergence in Møller–Plesset theory: A simple explanation based on a two-state model. *J. Chem. Phys.* **2000**, *112*, 9736–9748.

(31) Marie, A.; Burton, H. G. A.; Loos, P. F. Perturbation theory in the complex plane: exceptional points and where to find them. *J. Phys.: Condens. Matter* **2021**, *33*, 283001.

(32) Malrieu, J.-P.; Angeli, C. The Møller–Plesset perturbation revisited: origin of high-order divergences. *Mol. Phys.* **2013**, *111*, 1092–1099.

(33) Epstein, P. The Stark effect from the point of view of Schroedinger's quantum theory. *Phys. Rev.* **1926**, *28*, 695.

(34) Nesbet, R. Configuration interaction in orbital theories. *Proc. Roy. Soc. (London)* **1955**, *A230*, 312.

(35) Claverie, P.; Diner, S.; Malrieu, J. The Use of Perturbation Methods for the Study of the Effects of Configuration Interaction: I. Choice of the Zeroth-Order Hamiltonian. *Int. J. Quantum Chem.* **1967**, *1*, 751.

(36) Angeli, C.; Cimiraglia, R.; Malrieu, J.-P. On a mixed Møller–Plesset Epstein–Nesbet partition of the Hamiltonian to be used in multireference perturbation configuration interaction. *Chem. Phys. Letters* **2000**, *317*, 472–480.

(37) Szabo, A.; Ostlund, N. S. *Modern Quantum Chemistry*; McGraw-Hill: New York, 1989.

(38) Finley, J. P. Maximum radius of convergence perturbation theory. *J. Chem. Phys.* **2000**, *112*, 6997.

(39) Szabados, Á.; Surján, P. R. Optimized partitioning in Rayleigh-Schrödinger perturbation theory. *Chem. Phys. Letters* **1999**, *308*, 303.

(40) Surján, P. R.; Szabados, Á. Optimized partitioning in perturbation theory: comparison to related approaches. *J. Chem. Phys.* **2000**, *112*, 4438–4446.

(41) Surján, P. R.; Szabados, Á. Convergence enhancement in perturbation theory. *Collect. Czech. Chem. Commun.* **2004**, *69*, 105.

(42) Juhász, T.; Mazziotti, D. A. Improved perturbative treatment of electronic energies from a minimal-norm approach to many-body perturbation theory. *J. Chem. Phys.* **2005**, *122*.

(43) Mihálka, Z. É.; Szabados, Á.; Surján, P. R. Effect of partitioning on the convergence properties of the Rayleigh-Schrödinger perturbation series. *J. Chem. Phys.* **2017**, *146*, 124121.

(44) Shee, J.; Loipersberger, M.; Rettig, A.; Lee, J.; Head-Gordon, M. Regularized Second-Order Møller–Plesset Theory: A More Accurate Alternative to Conventional MP2 for Noncovalent Interactions and Transition Metal Thermochemistry for the Same Computational Cost. *J. Phys. Chem. Lett.* **2021**, *12*, 12084–12097.

(45) Finley, J. P.; Chaudhuri, R. K.; Freed, K. F. Applications of multireference perturbation theory to potential energy surfaces by optimal partitioning of H: Intruder states avoidance and convergence enhancement. *J. Chem. Phys.* **1995**, *103*, 4990.

(46) Forsberg, N.; Malmqvist, P.-Å. Multiconfiguration perturbation theory with imaginary level shift. *Chem. Phys. Letters* **1997**, *274*, 196.

(47) Witek, H. A.; Choe, Y.-K.; Finley, J. P.; Hirao, K. Intruder state avoidance multireference Møller–Plesset perturbation theory. *J. Comp. Chem.* **2002**, *23*, 957–965.

(48) Witek, H. A.; Nakano, H.; Hirao, K. Multireference perturbation theory with optimized partitioning. I. Theoretical and computational aspects. *J. Chem. Phys.* **2003**, *118*, 8197–8206.

(49) Battaglia, S.; Fransén, L.; Fdez. Galván, I.; Lindh, R. Regularized CASPT2: an Intruder-State-Free Approach. *J. Chem. Theory Comput.* **2022**, *18*, 4814–4825.

(50) Feenberg, E. Invariance Property of the Brillouin-Wigner Perturbation Series. *Phys. Rev.* **1956**, *103*, 1116.

(51) Goldhammer, P.; Feenberg, E. Refinement of the Brillouin-Wigner Perturbation Method. *Phys. Rev.* **1955**, *101*, 1233.

(52) Goodson, D. Convergent summation of Møller–Plesset perturbation theory. *J. Chem. Phys.* **2000**, *113*, 6461.

(53) Adams, W. H. Correction of Configuration-Interaction Wavefunctions by Perturbation Theory. *J. Chem. Phys.* **1966**, *45*, 3422.

(54) Fink, R. Two new unitary-invariant and size-consistent perturbation theoretical approaches to the electron correlation energy. *Chem. Phys. Letters* **2006**, *428*, 461.

(55) Dietz, K.; Schmidt, C.; Warken, M. Systematic construction of efficient many-body perturbation series. *J. Chem. Phys.* **1994**, *100*, 7421.

(56) Kelly, H. P. Correlation Effects in Atoms. *Phys. Rev.* **1963**, *131*, 684–699.

(57) Kelly, H. P. Many-Body Perturbation Theory Applied to Atoms. *Phys. Rev.* **1964**, *136*, B896–B912.

(58) Silver, D. M.; Bartlett, R. J. Modified potentials in many-body perturbation theory. *Phys. Rev. A* **1976**, *13*, 1–12.

(59) Freed, K. F. Is there a bridge between ab initio and semiempirical theories of valence? *Acc. Chem. Res* **1983**, *16*, 137–144.

(60) Finley, J. P.; Freed, K. F. Application of complete space multireference many-body perturbation theory to N_2: Dependence on reference space and H_0. *J. Chem. Phys.* **1995**, *102*, 1306.

(61) Chaudhuri, R. K.; Freed, K. F. Comparison of high order perturbative convergence of multireference perturbation methods: Application to singlet states of CH_2. *J. Chem. Phys.* **1997**, *107*, 6699.

(62) Carter-Fenk, K.; Head-Gordon, M. Repartitioned Brillouin-Wigner perturbation theory with a size-consistent second-order correlation energy. *J. Chem. Phys.* **2023**, *158*, 234108.

(63) Carter-Fenk, K.; Shee, J.; Head-Gordon, M. Optimizing the regularization in size-consistent second-order Brillouin-Wigner perturbation theory. *J. Chem. Phys.* **2023**, *159*, 171104.

(64) Knowles, P. J. Perturbation-adapted perturbation theory. *J. Chem. Phys.* **2022**, *156*, 011101.

(65) Amos, A. T.; Musher, J. I. Modified Hamiltonians for Localized Orbitals and for the Removal of Degeneracies. *J. Chem. Phys.* **1971**, *54*, 2380.

(66) S.Diner; J.-P.Malrieu; P.Claverie Localized bond orbitals and the correlation problem: I. The perturbation calculation of the ground state energy. *Theor. Chim. Acta* **1969**, *13*, 1,18.

(67) Davidson, E. R.; Bender, C. F. Unitary Transformations and Pair Energies. III. Relation to Perturbation Theory. *J. Chem. Phys.* **1972**, *56*, 4334.

(68) Davidson, E. R. Selection of the Proper Canonical Roothaan-Hartree-Fock Orbitals for Particular Applications. I. Theory. *J. Chem. Phys.* **1972**, *57*, 1999.

(69) Kapuy, E.; Bartha, F.; Bogár, F.; Kozmutza, C. Application of the many-body perturbation theory to normal saturated hydrocarbons in the localized representation. *Theor. Chim. Acta* **1987**, *72*, 337.

(70) Kapuy, E.; Bartha, F.; Kozmutza, C.; Bogár, F. The study of normal saturated hydrocarbons in the localized representation of the MBPT. *J. Mol. Struct. (THEOCHEM)* **1988**, *170*, 59.

(71) Kapuy, E.; Bartha, F.; Bogár, F.; Csépes, Z.; Kozmutza, C. Applications of the MBPT in the localized representation. *Int. J. Quantum Chem.* **1990**, *38*, 139.

(72) Kapuy, E.; Csépes, Z.; Kozmutza, C. Application of the many-body perturbation theory by using localized orbitals. *Int. J. Quantum Chem.* **1983**, *23*, 981–990.

(73) Kapuy, E.; Csépes, Z.; Kozmutza, C. Application of the many-body perturbation theory based on localized orbitals to cyclic polyenes. *Croatica Chemica Acta* **1984**, *57*, 855–864.

(74) Pipek, J.; Bogár, F. Many-Body Perturbation Theory with Localized Orbitals – Kapuy's Approach. *Top. Curr. Chem.* **1999**, *203*, 43.

(75) Surján, P. R.; Rolik, Z.; Szabados, Á.; Kőhalmi, D. Partitioning in multiconfiguration perturbation theory. *Ann. Phys. (Leipzig)* **2004**, *13*, 223–231.

(76) Surján, P. R.; Szabados, Á. In *Fundamental World of Quantum Chemistry, A Tribute to the Memory of Per-Olov Löwdin*; Brändas, E. J., Kryachko, E. S., Eds.; Kluwer: Dordrecht, 2004; Vol. III; pp 129–185.

(77) Subotnik, J. E.; Head-Gordon, M. A local correlation model that yields intrinsically smooth potential-energy surfaces. *J. Chem. Phys.* **2005**, *122*, 034109.

(78) Wilson, S.; Jankowski, K.; Paldus, J. Applicability of non-degenerate many-body perturbation theory to quasidegenerate electronic states: A model study. *Int. J. Quantum Chem.* **1983**, *23*, 1781–1802.

(79) Kaldor, U. Can nondegenerate many-body perturbation theory Be applied to quasidegenerate electronic states? *Int. J. Quantum Chem.* **1985**, *28*, 103.

(80) Wilson, S.; Jankowski, K.; Paldus, J. Applicability of nondegenerate many-body perturbation theory to quasi-degenerate electronic states. II. A two-state model. *Int. J. Quantum Chem.* **1985**, *28*, 525–534.

(81) Surján, P. R.; Kőhalmi, D.; Szabados, Á. Optimized quasiparticle energies in many-body perturbation theory. *Collect. Czech. Chem. Commun.* **2003**, *68*, 331–339.

(82) Surján, P. R.; Kőhalmi, D.; Szabados, Á. A note on perturbation-adapted perturbation theory. *J. Chem. Phys.* **2022**, *156*, 116102.

(83) Nesbet, R. Brueckner's Theory and the Method of Superposition of Configurations. *Phys. Rev.* **1958**, *109*, 1632.

(84) Handy, N. C.; Pople, J. A.; Head-Gordon, M.; Raghavachari, K.; Trucks, G. W. Size-consistent Bruckner theory limited to double substitutions. *Chem. Phys. Letters* **1989**, *164*, 185.

(85) Surján, P. R.; Szabados, Á. Many-Body Perturbation Theory with Localized Orbitals: Accounting for Localization Diagrams as Integral Dressing. *J. Chem. Theory Comput.* **2022**, *18*, 2955–2958.

(86) Bisgard, J. *Analysis and Linear Algebra: The Singular Value Decomposition and Applications*; American Mathematical Society: Rhode Island, 2021.

(87) Cahill, K. *Physical Mathematics*; Cambridge University Press: United Kingdom, 2013; Chapter 1.31.

(88) Szabados, Á.; Surján, P. R. Size dependence of Feenberg scaling. *Int. J. Quantum Chem.* **2005**, *101*, 287–290.

(89) Dunning, T. Gaussian basis sets for use in correlated molecular calculations. I. The atoms boron through neon and hydrogen. *J. Chem. Phys.* **1989**, *90*, 1007.

(90) Huber, K. P.; Herzberg, G. *Molecular Spectra and Molecular Structure*; Springer US, 1979.

(91) Chang, S. Y. Accurate Calculation of the Vibrational Force Constant of the Hydrogen Molecule by Variation–Perturbation Theory. *J. Chem. Phys.* **1972**, *56*, 4–7.

(92) Purvis, G. D.; Shepard, R.; Brown, F. B.; Bartlett, R. J. C_{2v} Insertion pathway for BeH_2: A test problem for the coupled-cluster single and double excitation model. *Int. J. Quantum Chem.* **1983**, *23*, 835–845.

(93) Krishnan, R.; Binkley, J.; Seeger, R.; Pople, J. Self-consistent molecular orbital methods. XX. A basis set for correlated wave functions. *J. Chem. Phys.* **1980**, *72*, 650.

(94) Boys, S.; Bernardi, F. The calculation of small molecular interactions by the differences of separate total energies. Some procedures with reduced errors. *Mol. Phys.* **1970**, *19*, 553–566.

TOC Graphic